The EMBO Journal Vol.18 No.3 pp.522–533, 1999

Retrograde Ca^{2+} signaling in C2C12 skeletal myocytes in response to mitochondrial genetic and metabolic stress: a novel mode of inter-organelle crosstalk

Gopa Biswas, Olugbenga A.Adebanjo[1], Bruce D.Freedman, Hindupur K.Anandatheerthavarada, C.Vijayasarathy, Mone Zaidi[1], Michael Kotlikoff and Narayan G.Avadhani[2]

Department of Animal Biology, and the Mari Lowe Center for Comparative Oncology, School of Veterinary Medicine, University of Pennsylvania, Philadelphia, PA 19104 and [1]Division of Geriatrics and Extended Care Service, The Veterans Affairs Medical Center, University and Woodland Avenue, Philadelphia, PA 19104, USA

[2]Corresponding author
e-mail: narayan@vet.upenn.edu

O.A.Adebanjo, B.D.Freedman and H.K.Anandatheerthavarada contributed equally to this work

We have investigated the mechanism of mitochondrial–nuclear crosstalk during cellular stress in mouse C2C12 myocytes. For this purpose, we used cells with reduced mitochondrial DNA (mtDNA) contents by ethidium bromide treatment or myocytes treated with known mitochondrial metabolic inhibitors, including carbonyl cyanide *m*-chlorophenylhydrazone (CCCP), antimycin, valinomycin and azide. Both genetic and metabolic stresses similarly affected mitochondrial membrane potential ($\Delta\psi_m$) and electron transport-coupled ATP synthesis, which was also accompanied by an elevated steady-state cytosolic Ca^{2+} level ($[Ca^{2+}]_i$). The mitochondrial stress resulted in: (i) an enhanced expression of the sarcoplasmic reticular ryanodine receptor-1 (RyR-1), hence potentiating the Ca^{2+} release in response to its modulator, caffeine; (ii) enhanced levels of Ca^{2+}-responsive factors calineurin, calcineurin-dependent NFATc (cytosolic counterpart of activated T-cell-specific nuclear factor) and c-Jun N-terminal kinase (JNK)-dependent ATF2 (activated transcription factor 2); (iii) reduced levels of transcription factor, NF-κB; and (iv) enhanced transcription of cytochrome oxidase Vb (*COX Vb*) subunit gene. These cellular changes, including the steady-state $[Ca^{2+}]_i$ were normalized in genetically reverted cells which contain near-normal mtDNA levels. We propose that the mitochondria-to-nucleus stress signaling occurs through cytosolic $[Ca^{2+}]_i$ changes, which are likely to be due to reduced ATP and Ca^{2+} efflux. Our results indicate that the mitochondrial stress signal affects a variety of cellular processes, in addition to mitochondrial membrane biogenesis.

Keywords: Ca^{2+} signaling/membrane potential/mitochondrial DNA/ryanodine receptor/stress response

Introduction

Mitochondrial membrane biogenesis involves a complex cooperative interaction between protein subunits encoded by both the nuclear and mitochondrial genes (Attardi and Schatz, 1988; Poyton and McEwen, 1996). Although relatively small in number, mitochondrial-encoded proteins play crucial roles in either the catalytic function or assembly of mitochondrial electron transport chain complexes (Attardi and Schatz, 1988; Capaldi, 1990). The critical role of mitochondrial gene products in the mitochondrial membrane biogenesis is further illustrated by the discovery of a heterogeneous group of diseases, collectively termed mitochondrial myopathies and encephalopathies, which are characterized by mitochondrial DNA (mtDNA) mutations and altered electron transport chain-coupled oxidative phosphorylation (Wallace, 1992; DiMauro, 1993, 1996). The genetic lesions in these patients include point mutations in the tRNA or protein coding genes such as in *MERRF* (myoclonal epilepsy ragged Red Fiber) and *KSS* (Kearn–Sayre syndrome) and deletions of 1–8 kb region of mtDNA, in LOHN (Leber's hereditary optic neuropathy) patients (Holt *et al*., 1988; Wallace *et al*., 1988; Moraes *et al*., 1989; Corral-Debrinski *et al*., 1992). Accumulation of mitochondrial mutations and associated changes in the mitochondrial NADH–ubiquinone oxidoreductase and cytochrome *c* oxidase complexes have been reported in age-related idiopathic Parkinson's disease, Alzheimer's disease and also in ageing *per se* (Arnheim and Cortopassi, 1992; Hayakawa *et al*., 1992; Davis *et al*., 1997). Because of the heteroplasmy of mtDNA population in affected cells, a threshold accumulation of mutated DNA, affecting the functions of the mitochondrial energy transducing complexes and cellular ATP production, is thought to be the primary cause of these varied neuro–muscular–retinal degenerative diseases (Arnheim and Cortopassi, 1992; Wallace, 1992; DiMauro, 1993).

A number of studies also suggest that the state of mtDNA or its level of expression may affect nuclear gene expression, and thus mitochondrial biogenesis. Early studies in *Neurospora crassa* showed that treatment of cells with mitochondrial-specific transcription and/or translation inhibitors resulted in elevated levels of nuclear-encoded RNA polymerase and tRNA synthetase in the mitochondrial compartment (Barath and Kuntzel, 1972). These and related studies (Kuiper *et al*., 1988; for a review see Poyton and McEwen, 1996) led to an interesting but unresolved hypothesis that mitochondrial-encoded factor(s), transported to the nucleus, may regulate the transcription of a number of nuclear genes which code for various mitochondrial proteins (Barath and Kuntzel, 1972; reviewed in Nagley, 1991; Poyton and McEwen, 1996; Lenka *et al*., 1998). More recent studies (Parikh *et al*., 1987; Liao and Butow, 1993) demonstrated that respiratory-deficient yeast cells, which lack mtDNA (ρ^o cells), contain 20- to 30-fold increased levels of nuclear-specified RNAs mapping to gene loci, designated as class I genes (reviewed in Poyton and McEwen, 1996). In an

important series of experiments, Butow and coworkers showed that upregulation of the *CIT2* gene, a member of class I gene family, in ρ^o yeast cells involves the activation of a novel bHLH zip transcription factor, which binds to specific *cis* DNA sequences of target genes (Rothermel *et al*., 1995; Jia *et al*., 1997). The functional activation of the factor requires at least three gene products, Rtg1p, Rtg2p and Rtg3p; the first two being subunits of the dimeric bHLH factor, and the third being a member of the heat shock protein (HSP) family of proteins, which regulates the activity of the factor. It is hypothesized that the activation of the bHLH factor occurs through a 'retrograde pathway' which is possibly a stress response signal to mitochondrial dysfunction. However, the precise details of the retrograde pathway with respect to the nature of signals transmitted from the mitochondrial compartment to the nucleus or the mode of its transmission remain unclear. Furthermore, currently there is very little evidence for the occurrence of such a mitochondria-to-nucleus retrograde signaling in vertebrate cells.

In the present study, to address the question of retrograde signaling in vertebrate cells and also to evaluate the role of this signaling on cell differentiation, we have developed C2C12 muscle cell lines containing varying levels of mtDNA, by long-term exposure to ethidium bromide (EtBr). The ability to reverse the mtDNA level in these mutant cells following removal of EtBr provides a useful model system to study cellular processes affected by changes in mtDNA dosage, and also the mechanisms of mitochondrial myopathies associated with mtDNA ablation. Our results show that depletion of mtDNA below a certain threshold level or disruption of $\Delta\psi_m$ by mitochondrial inhibitors results in: (i) increased basal Ca^{2+}, possibly due to reduced ATP levels affecting Ca^{2+} efflux; (ii) enhanced expression of the gene for ryanodine receptor-1 (*RyR-1*) Ca^{2+} release channel; and (iii) altered activities of three different Ca^{2+}-dependent transcription factor pathways. Most notably, normalizing the mtDNA content readily reverses all of these changes. These results therefore describe a classical retrograde Ca^{2+} signaling from mitochondria-to-nucleus, that can potentially affect not only genes important for mitochondrial function, but also a number of nuclear genes with varied cellular functions.

Results

Development of C2C12 cell lines with partially depleted mtDNA

Phenanthredine dye, EtBr, is known to selectively inhibit mtDNA replication and transcription (Nass, 1972), and has been used to develop avian and human cell lines devoid of mtDNA (Desjardines *et al*., 1986; King and Attardi, 1989). It is widely believed that long-term treatment with low doses of EtBr leads to selective loss of mtDNA without detectable effects on the nuclear DNA. In our initial attempts, C2C12 muscle cells exposed to EtBr for as many as 70 cycles of growth yielded a mixed population of cells containing varying levels of mtDNA. From this mixed population of cells, we isolated ~30 individual clones by single cell selection, and chose three of these clones, designated as clones 2, 10 and 23 for further characterization. Southern blot hybridization of total cell DNA in Figure 1A shows that clones 10 and 23 contain reduced mtDNA contents in the range of between ~80 and 50% of the normal untreated cells, respectively (lanes 2 and 4). Clone 2 represents the most severely depleted cell line with only ~20% of the mtDNA content compared with normal untreated cells (Figure 1A, lanes 3 and 1). Results also show that the mtDNA content of the reverted cell line, which is essentially clone 2 grown for 50 division cycles in the absence of added EtBr, is restored to ~90% of the control cell level (Figure 1A, lane 5). The variability of mtDNA content of different clones between experiments was minimized by using cells from the same frozen stock for all the experiments. Cells were grown in the presence of EtBr for no more than 4 days, and the mtDNA contents were monitored routinely.

Figure 1B shows the Northern blot analysis of mtDNA-encoded cytochrome oxidase subunit I (COX I) mRNA in control and depleted cells. Consistent with the relative mtDNA contents of these cell lines, the Northern blot data show that clone 2 contains only ~20% COX I mRNA as detected in normal cells (Figure 1B, lanes 3 and 1). Clones 10 and 23 contain 60 and 50% of the normal cell level (Figure 1B, lanes 2 and 4). The reverted cell line, on the other hand, contains ~85% of the normal untreated controls (Figure 1B, lane 5). Immunohistograms in Figure 1C using monoclonal antibody to human COX I protein show that clone 2 contains very low levels of antibody reactive protein (panel c), while clone 10 contains a level intermediary between the normal cell mitochondria and most depleted clone 2 (panel b). Although not shown, clone 23 exhibited levels comparable to clone 10, and the reverted cells contained near normal levels of antibody-cross reacting COX I protein (panel d). These results show that the three depleted clones and the reverted clone contain different levels of mtDNA, and also varying levels of mitochondrial gene products, that are consistent with their DNA contents.

The reversible effects of mtDNA depletion on mitochondrial membrane potential was tested using a cationic fluorescent dye 'Mitotracker' whose mitochondrial localization is highly dependent on the inside-out voltage difference in membrane potential (Chen, 1989). Figure 1D shows that normal cells can efficiently mobilize the dye in mitochondria-like punctuate structures (panel a), while clone 10 and clone 2 cells show vastly reduced fluorescence suggesting disrupted $\Delta\psi_m$ (panels b and c). As expected from the recovery of the mtDNA level, the reverted cells show near normal intensity of fluorescence suggesting re-establishment of mitochondrial membrane potential (panel d). Immunostaining with antibody against nuclear-encoded COX VIc protein (Figure 1E), on the other hand, yielded nearly comparable staining in both control (panel a) and mtDNA-depleted cells (panels b and c), suggesting near normal mitochondrial morphology in the mutant cells. Thus, the results of mtDNA analysis, together with the biochemical characteristics of these cell lines ascertain the complete reversibility of the system.

Reversible effects of mtDNA depletion on ATP level and steady-state $[Ca^{2+}]_i$

The total cellular ATP and mitochondrial respiration-coupled ATP [measured as carbonyl cyanide *m*-chlorophenylhydrazone (CCCP) or oligomycin-sensitive ATP]

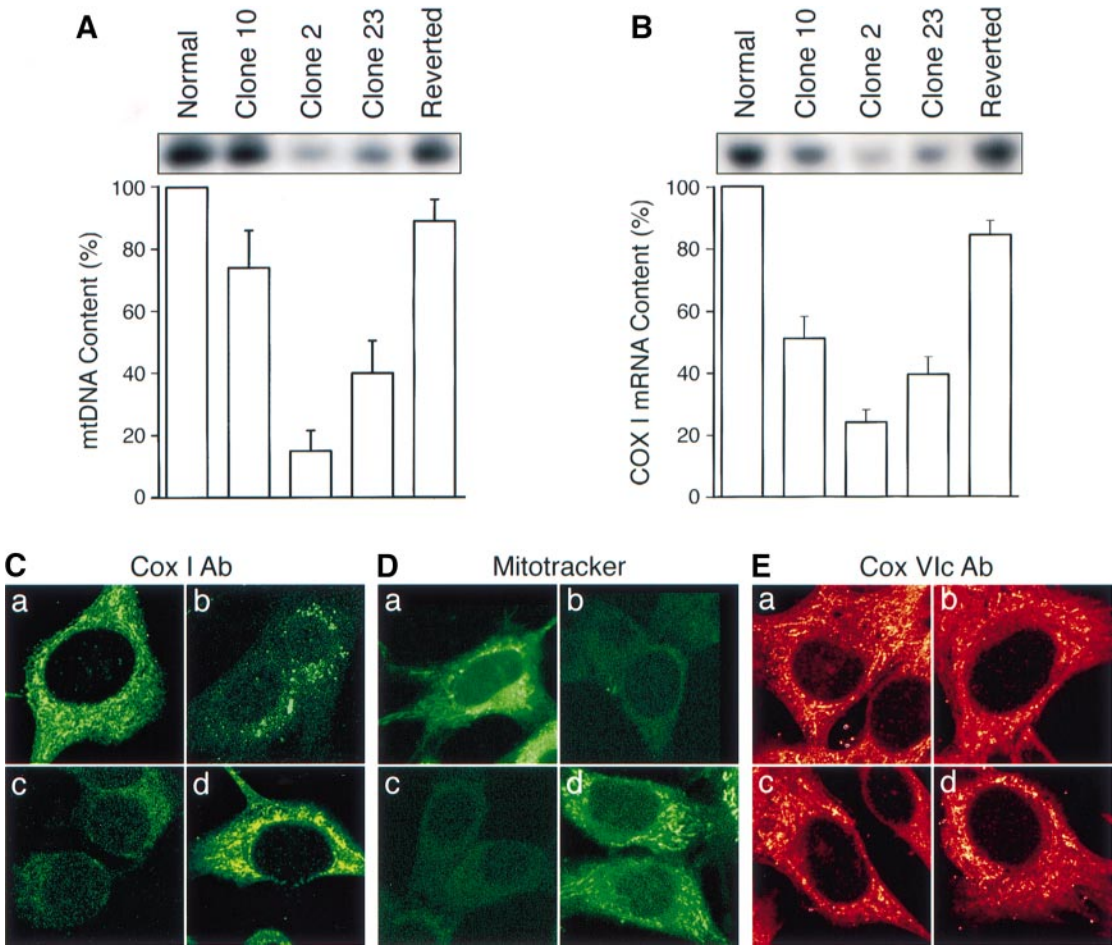

Fig. 1. mtDNA contents and membrane characteristics of different clones. (**A**) mtDNA contents of clones 2, 10 and 23, as well as Reverted, were determined by Southern blot hybridization with a 5′ end labeled COX I-specific DNA probe described in Materials and methods. The blot was imaged and quantitated in a Bio-Rad GS-525 imager and reprobed with ^{32}P-labeled DNA probe for 18S rRNA. The mtDNA level of each sample was normalized to the 18S DNA content. (**B**) mtDNA-encoded COX I mRNA contents of different clones. Total RNA (30 μg) from each of the control and mtDNA-depleted clones were subjected to Northern blot hybridization with ^{32}P-end labeled COX I DNA probe as in (A). (**C**) Immunofluorescence patterns of cells stained with monoclonal antibody against mitochondrial gene coded COX I subunit; (**D**) live cells stained with 400 nM cationic dye, Mitotracker (Molecular Probes, Inc.) according to the manufacturer's suggested protocol, and fixed with 2% paraformaldehyde; and (**E**) immunofluorescence patterns of cells stained with monoclonal antibody against nuclear gene-encoded COX Vc subunit. (C, D and E): (a) control cells; (b) least mtDNA-depleted clone 10; (c) most mtDNA-depleted cone 2; and (d) reverted clone. Staining with primary and secondary antibodies and Mitotracker dye, and confocal microscopy were as described in Materials and methods.

were determined using the ATP-driven luciferase assay (Strehler, 1968). Figure 2A shows that the total cellular ATP in clone 10 and clone 2 were reduced, respectively, to ~75 and ~45% of the control cell level. Approximately 50% of the ATP pool in control cells was sensitive to pre-treatment with CCCP or oligomycin, suggesting that it may represent the respiration-coupled component of the cell. As expected, the CCCP or oligomycin-sensitive components in clone 10 and clone 2 were progressively reduced to ~40 and >10% of the total cell ATP. Although not shown, the ATP levels of reverted cells were similar to those of control cells. These results suggest that the mtDNA-depleted cell lines have impaired mitochondrial oxidative phosphorylation, but a near normal glycolytic and other alternate energy generating pathways.

Results from various laboratories have shown that mitochondria accumulate Ca^{2+} during physiological stimulation resulting in intracellular calcium release (Carafoli, 1979; Rizzuto *et al*., 1993; Loew *et al*., 1994; Hajnoczky *et al*., 1995). Subsequent opening of permeability transition pores releases mitochondrial calcium, directly producing calcium release transients (Altshuld *et al*., 1992; Friel and Tsien, 1994; Ichas *et al*., 1994, 1997; Babcock *et al*., 1997). Calcium uptake into the mitochondria by the H^+ uniporter and calcium release are functions of $\Delta\psi_m$, which varies during calcium release and provides the electrochemical gradient driving calcium flux (Ichas *et al*., 1997). Since the mtDNA-depleted cells in the present study showed altered $\Delta\psi_m$, and altered ATP levels, we measured steady-state $[Ca^{2+}]_i$ by digital imaging of single fura-2-loaded myocytes. Results in Figure 2B show basal $[Ca^{2+}]_i$ values (mean ± SEM) from 35–72 randomly selected cells. It is seen that control untreated cells show basal levels of 65 ± 4.3 nM (first bar), which was significantly higher [$p < 0.01$, by analysis of variance (ANOVA)] in the mtDNA-depleted clone 10 (116 ± 8.4 nM) and clone 2 (147 ± 5.7 nM) (second and third bars). The mean $[Ca^{2+}]_i$ level of reverted cells was however not significantly different from untreated control cells (75 ± 4.5 nM) (fourth bar). In view of current

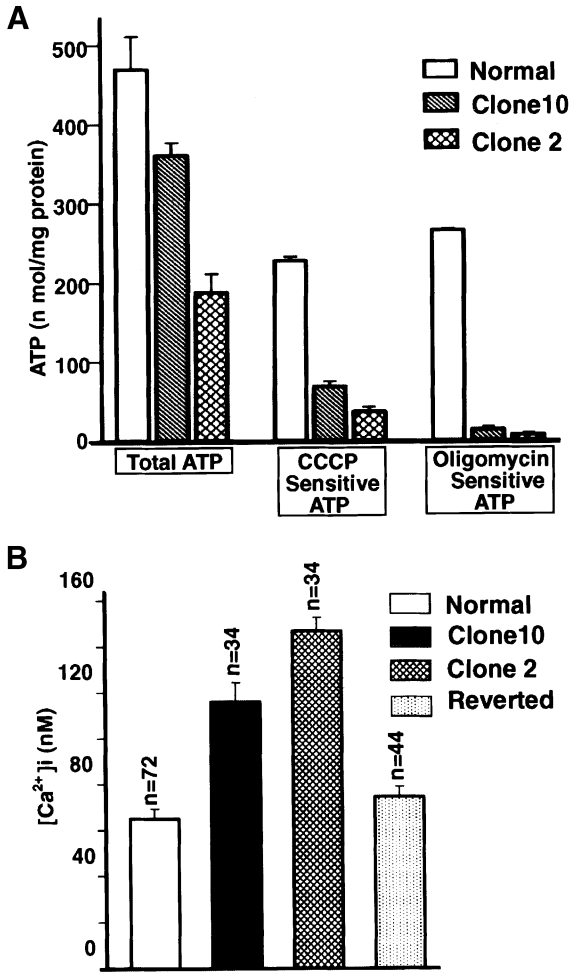

Fig. 2. Reduced cellular ATP and elevated steady-state $[Ca^{2+}]_i$ in mtDNA-depleted cells. (**A**) ATP levels were measured by the luciferin luciferase assay method as described in Materials and methods. The values obtained with cells treated with CCCP (20 μM) or oligomycin (25 μM) for 30 min were subtracted from the control cell ATP to obtain the CCCP-sensitive and oligomycin-sensitive components, respectively. (**B**) The steady-state $[Ca^{2+}]_i$ from mtDNA-depleted and reverted cells were measured in fura-2-loaded cells as described in Materials and methods.

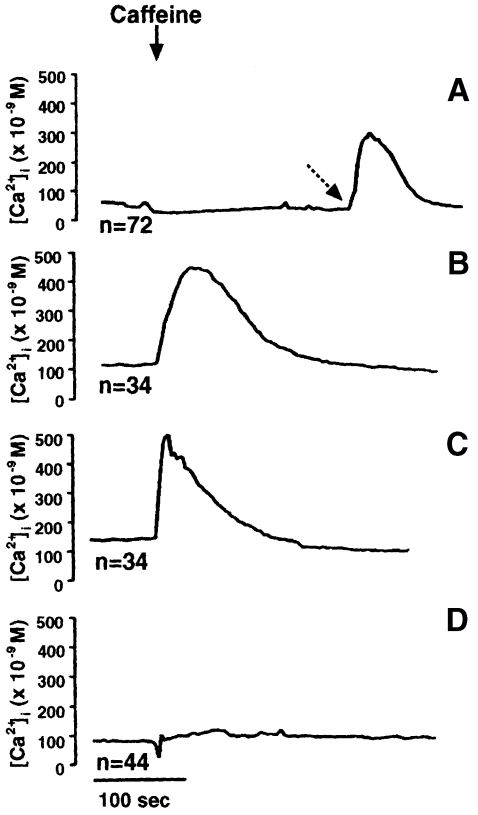

Fig. 3. Caffeine-mediated Ca^{2+} release in single myocytes. Caffeine (20 mM) was added at the indicated time (solid arrow) in all cases. In panel (A), 1 mM acetylcholine was added at 310 s as a control for stored Ca^{2+} as indicated by the dotted arrow. (**A**) Control untreated cells (caffeine evoked $[Ca^{2+}] = 40 \pm 2.8$ nM, acetylcholine evoked peak $[Ca^{2+}] = 279 \pm 17.3$ nM, $n = 72$ cells); (**B**) clone 10 (caffeine evoked peak $[Ca^{2+}] = 476 \pm 50.3$ nM, $n = 34$ cells); (**C**) clone 2 (caffeine evoked peak $[Ca^{2+}] = 504 \pm 45.4$, $n = 34$ cells), and (**D**) reverted clone ($n = 44$ cells).

dogma that Ca^{2+} influx (via channels) and efflux (into storage vesicles or across the plasma membrane) are the primary determinants of cellular steady-state $[Ca^{2+}]_i$, our results imply that altered $\Delta\psi_m$ and reduced cellular ATP level may result in reduced Ca^{2+} efflux, thus establishing a new steady-state (basal) $[Ca^{2+}]_i$.

Ryanodine receptor Ca^{2+} channel levels in mtDNA-depleted and reverted cells

Prompted by the elevated steady-state $[Ca^{2+}]_i$ in mtDNA-depleted cells, we decided to investigate the nature of caffeine and $InsP_3$(inositol 1,4,5 triphosphate)-responsive internal Ca^{2+} stores. Strikingly, although normal cells did not respond to caffeine (Figure 3A), consistent with low expression of RyRs in undifferentiated myocytes (Bennett *et al*., 1996), exposure of mtDNA-depleted clones resulted in a marked $[Ca^{2+}]_i$ transient (Figure 3B and C), suggesting functional RyR expression. Peak calcium transients were 476 ± 50.3 and 504 ± 45.4 nM in the least depleted and most depleted clones, respectively (Figure 3B and C). The lack of response to caffeine in normal cells was not associated with an absence of intracellular calcium stores; acetylcholine, which releases Ca^{2+} through the generation of $InsP_3$ in these cells (Grassi *et al*., 1993), provoked marked $[Ca^{2+}]_i$ transients (Figure 3A). Interestingly, as with control cells, caffeine also failed to elicit calcium release in reverted cells (Figure 3D).

Caffeine increases the affinity of RyRs for Ca^{2+} ions, resulting in RyR-channel gating at resting $[Ca^{2+}]_i$. The induction of caffeine-stimulated Ca^{2+} release in mtDNA-depleted cells suggested either an increased expression of RyR receptor protein, or alteration in caffeine sensitivity of expressed RyRs either by a post-translational activation of the receptor protein, or a shift in isoform expression. We investigated these possibilities by assessing the RyR protein levels by immunohistochemical analysis and also by Western blot analysis using an affinity-purified antibody raised to purified RyR-1 (Zaidi *et al*., 1995). The immunohistograms in Figure 4A show a vastly increased fluorescence in the mtDNA-depleted cells (panels b and c) compared with untreated control myocytes (panel a). The reverted cells (panel d), on the other hand, showed an intensity close to the control cells. Although not shown, all three cell lines yielded similar fluorescence intensity when stained with antibody to Na^+/K^+ ATPase. The Western blots in Figure 4B show that the post-nuclear

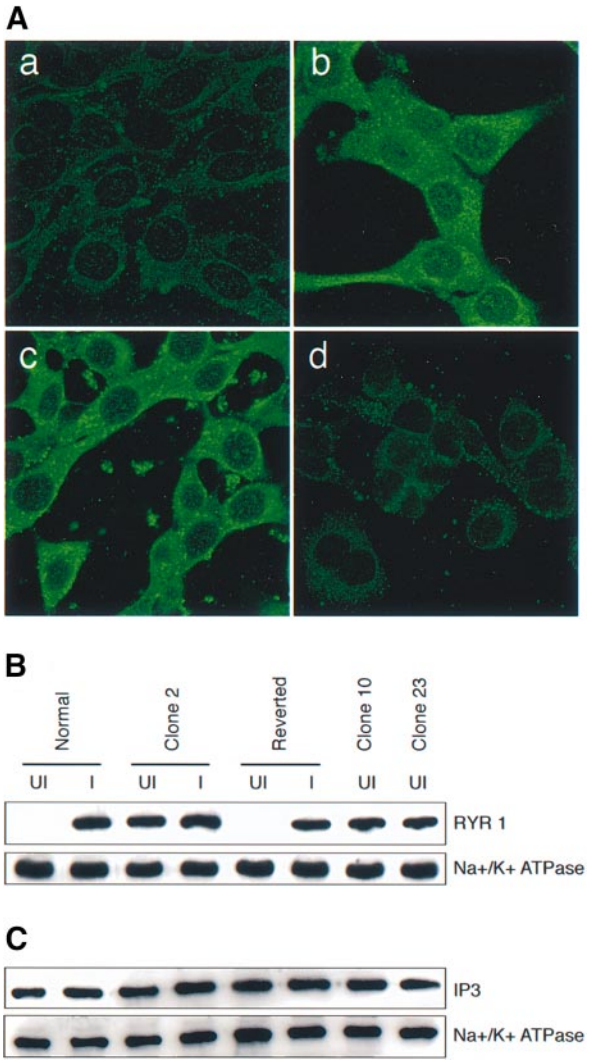

Fig. 4. Increased RyR-1 receptor protein levels in mtDNA-depleted cells. (**A**) Paraformaldehyde-fixed, and Triton permeabilized cells were stained with affinity-purified RyR-1 antibody as described in Materials and methods. (**B** and **C**) Western blot analyses with antibodies to RyR-1 and IP3 receptor proteins, respectively. Post-nuclear fractions of cells (50 μg each) from undifferentiated (UI) and induced by serum withdrawal (I) were resolved on 5% polyacrylamide gels. The blots were co-developed with antibody to Na^+/K^+ ATPase as an internal loading control.

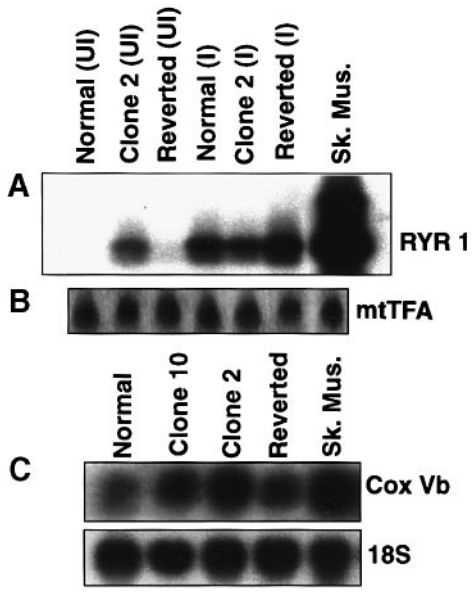

Fig. 5. Increased levels of nuclear-encoded RyR-1 and COX Vb mRNAs in mtDNA-depleted cells. (**A**) Increased steady-state levels of RyR-1 mRNA in mtDNA-depleted cells. Reverse transcriptase-based PCR products, generated by using RyR-1 mRNA-specific primers and total RNAs from various cells and mouse skeletal muscle (Sk. Mus.) were probed with ^{32}P-labeled RyR-1 DNA probe. A 530 bp DNA corresponding to sequence 14434–14967 of rabbit RYR-1 cDNA was used as the probe (Bennett *et al*., 1996). (**B**) Levels of mtTFA mRNA in control and mtDNA-depleted cells. Companion RT–PCR reactions as in (A) were run using the mouse mtTFA primers as controls, and the products were subjected to Southern blot hybridization with ^{32}P-labeled mouse mtTFA probe (Larsson *et al*., 1996). (**C**) Levels of nuclear-encoded mRNA for mitochondrial COX Vb subunit. Total RNA from various cells (30 μg each) were subjected to Northern blot hybridization with ^{32}P-labeled mouse COX Vb cDNA probe. The blot was co-hybridized with a ^{32}P-labeled 18S DNA probe.

fraction from untreated control cells (lane 1) contains no significant characteristic >500 kDa immunoreactive protein, while clones 10, 2 and 23 (lanes 3, 7 and 8) with different levels of mtDNA depletion show distinct high molecular weight RyR-1 protein. Interestingly, the reverted clone appears similar to the untreated control (Figure 4B, lane 5), in that it contains no detectable immunoreactive >500 kDa RyR-1 protein. As expected, induced myogenesis in both normal and reverted cells (Figure 4B, lanes 2 and 6) caused induction of RyR-1 antibody reactive protein. Serum withdrawal for the induction of myogenesis in clone 2 (Figure 4B, lane 4) had no effect on the level of RyR-1 protein. All four of the cell lines however contained similar levels of Na^+/K^+ ATPase, which was used as an internal loading control. Consistent with the caffeine-mediated Ca^{2+} release data in Figure 3, these Western blot results demonstrate that in mtDNA-depleted cells, there is a reversible elevation of RyR-1 receptor protein. The Western blot data in Figure 4C also show that the level of IP3-sensitive Ca^{2+} channel protein remains relatively the same in both the control and various mtDNA-depleted cells. Although not presented, a generally low, yet similar levels of RyR-3 antibody reactive protein was detected in control, mtDNA-depleted and reverted myocytes, suggesting the specificity of nuclear gene targets affected by the mtDNA depletion.

The possibility of transcriptional upregulation of *RyR-1* gene expression in mtDNA-depleted cells was investigated by a quantitative reverse transcriptase-based PCR method. Recently, Bennett *et al*. (1996) used a set of degenerate primers to show that both *RyR-1* and *RyR-3* gene expression were markedly induced in differentiated C2C12 myoblasts. In our hands, the degenerate primers did not yield significant amplification of either of the mRNAs. We have therefore used rabbit muscle RyR-1 specific primers (Takeshima *et al*., 1989), which yielded a single PCR product with the induced C2C12 myocyte RNA (Figure 5A, lane 4) and two distinct PCR products with the mouse skeletal muscle RNA (lane 7). The 530 bp band from both sources was sequenced and found to be RyR-1 specific. Based on the nucleotide sequence data, the slower migrating skeletal muscle-specific product appears to be Ca^{2+}-channel related, although its precise classification will require additional characterization. In Figure 5A the products of quantitative PCR were hybrid-

ized with mouse skeletal muscle RyR-1-specific DNA sequence. In support of Bennett *et al*. (1996), undifferentiated C2C12 myoblasts contained no detectable RyR-1-specific RNA (Figure 5A, lane 1) while differentiated myotubes contained vastly induced RyR-1 mRNA (Figure 5A, lane 4). Interestingly, myoblasts depleted of mtDNA showed induced expression of RyR-1 mRNA (Figure 5A, lane 2). Growth of mtDNA-depleted cells under conditions that normally induce myoblasts to form myotubes had no effect on the mRNA level (Figure 5A, lane 5). Finally, the reverted cells also showed very low RyR-1 mRNA content (Figure 5A, lane 3) which was induced several fold by induced myogenesis (lane 6). In Figure 5B, Southern blot hybridization of RT–PCR products of mtTFA (mitochondrial transcription factor A) mRNA (Larsson *et al*., 1996), used as an internal control is shown. These controls show no significant mRNA variation in these cells under both normal and serum-deprived growth conditions. Figure 5C shows the Northern blot analysis of total RNA from various depleted and reverted C2C12 cell lines with a DNA probe for nuclear-encoded cytochrome oxidase subunit Vb (COX Vb) mRNA. Results show that COX Vb mRNA levels are also induced 4- to 7-fold in mtDNA-depleted cells (Figure 5C, lanes 2 and 3) compared with the normal cells (lane 1). The reverted cells showed 2- to 3-fold lower mRNA content (Figure 5C, lane 4) compared with mtDNA-depleted clone 2 (lane 3). These results demonstrate for the first time that mtDNA depletion results in an elevated expression of sarcoplasmic reticular RyR-1 Ca^{2+} channel mRNA in addition to mRNA for mitochondrial destined COX Vb protein. Results of nuclear run on experiments (data not shown) show that the observed increase is due to transcriptional upregulation.

Effects of mtDNA depletion on Ca^{2+}-related transcription factors

It is now well established that hormone or agonist-mediated Ca^{2+} release from internal stores or outside the cell results in the differential activation of various pro-inflammatory transcription regulatory factors as end points of signal cascade (Liu *et al*., 1991; O'Keefe *et al*., 1992; Clapham 1995; Dolmetsch *et al*., 1997). We have therefore investigated the state of three different inflammatory response pathway factors, namely NF-κB, calcineurin-dependent NFAT (activated T-cell specific nuclear factor) and c-Jun N-terminal kinase (JNK)-dependent ATF2 (also referred to as CREBP1) factors as a consequence of mtDNA depletion and reversion.

Western blot results in Figure 6A show that the level of IκB, the cytoplasmic inhibitor which binds and inhibits the translocation of NF-κB (Sen and Baltimore, 1986; Grilli *et al*., 1993) is induced in mtDNA-depleted cells compared with the control. Interestingly, reverted cells show reduced IκB levels consistent with the untreated cells. Conversely, the level of RelA, the activated form of NF-κB (Grilli *et al*., 1993) in the nucleus is reduced in mtDNA-depleted cells, and increased in the control, as well as in the reverted cell nuclei (see Figure 6D). We also determined the level of p50, the second component of the heterodimeric NF-κB factor (Fan and Maniatis, 1991), and surprisingly found that the nuclear levels of this protein (Figure 6E) in mtDNA-depleted cells is increased 2- to 2.5-fold. Although not presented, the levels

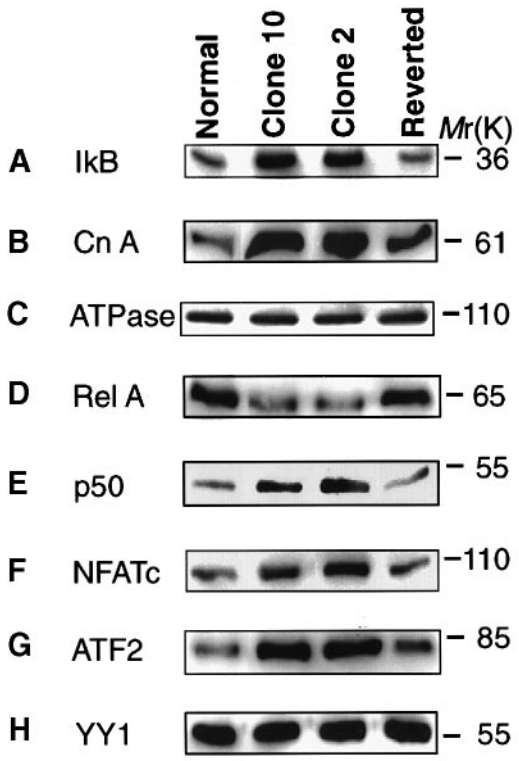

Fig. 6. Reversible activation or inactivation of nuclear transcription factors in mtDNA-depleted cells. (**A** and **B**) Western blot analyses of post-nuclear fractions (50 μg each) with antibody to IκB α and calcineurin A subunit, respectively. (**C**) The blot in (A) was co-developed with antibody to Na^+/K^+ ATPase as an internal loading control. (**D**–**G**) Twenty micrograms each of nuclear proteins were probed with antibodies to Rel A, p50, NFATc and Tyr phosphorylated ATF2, respectively. These blots were also co-developed with antibody to transcription factor YY-1 as an internal control, and a representative blot has been presented in (**H**). The blots were imaged and quantitated in a Bio-Rad Fluor-S imaging system.

of RelB and p52 proteins remained relatively same in mtDNA-depleted cells. Based on the current notion that the RelA/p50 heterodimeric factor is a transcriptional activator, while p50 homodimer is a transcriptional repressor, our results indicate a change in the composition and possibly a reduced activity of NF-κB family factors in mtDNA-depleted cells.

Calcineurin is a cytoplasmic, Ca^{2+}-dependent, protein phosphatase, which is implicated in Ca^{2+}-mediated signaling in T cell activation, inflammatory response, apoptosis and cardiac hypertrophy (Shibasaki and McKeon, 1995; Molkentin *et al*., 1998). Calcineurin consists of a catalytic subunit CnA, which dephosphorylates target proteins belonging to NFAT family of transcription factors, such as NFATc, thus activating their nuclear translocation (Shibasaki *et al*., 1996). Calcineurin also contains a regulatory subunit, CnB, which modulates the activity of the catalytic subunit (Milan *et al*., 1994). Figure 6B shows that the steady-state levels of the catalytic subunit CnA in the post-mitochondrial fraction of mtDNA-depleted clone 2 and 10 is induced ~10-fold, and returned to near normal levels (2- to 3-fold of normal) in reverted cells. Although results are not presented, the level of the CnB was also increased marginally in mtDNA-depleted cells. In contrast, the level of the Na^+/K^+ ATPase protein used as an internal control remained nearly the same in

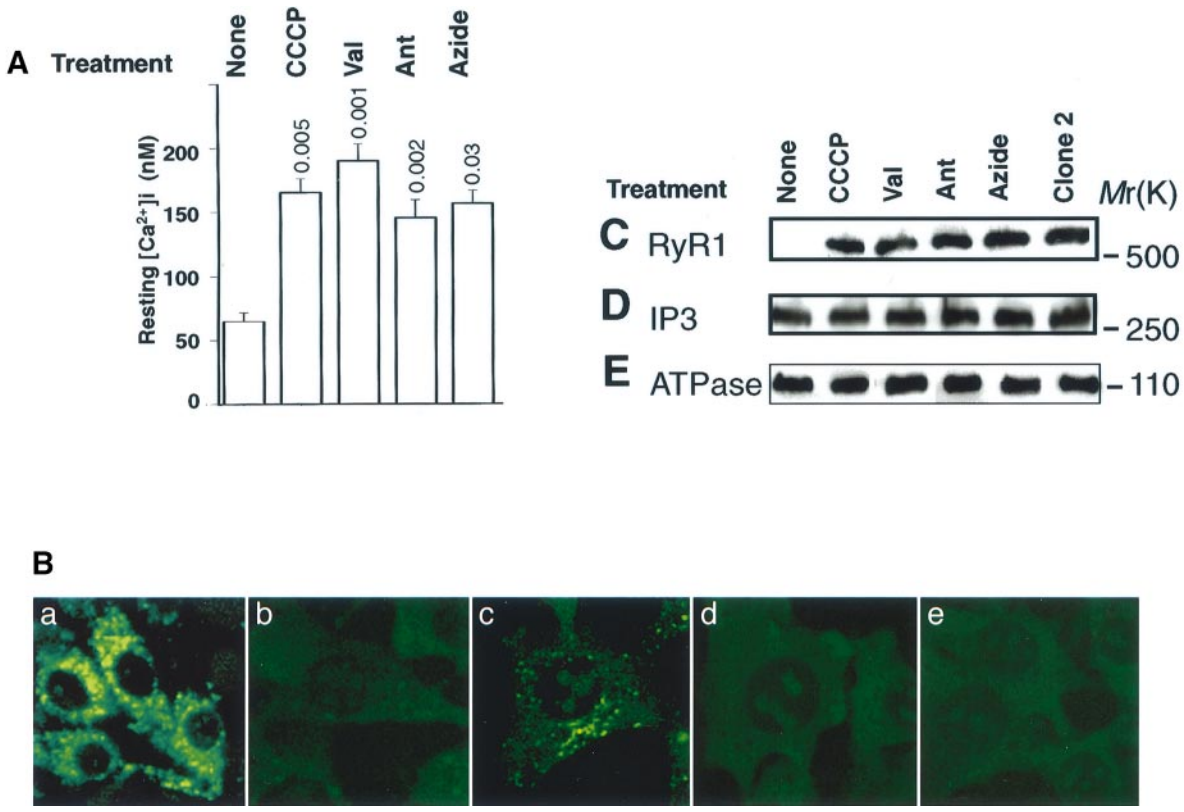

Fig. 7. Effects of metabolic inhibitors on $\Delta\psi_m$, steady-state $[Ca^{2+}]_i$ and RyR-1 expression. (**A**) Resting $[Ca^{2+}]_i$ was measured in fura-2-loaded control and inhibitor-treated cells as described in Materials and methods. Treatment was carried out for 30 min with CCCP (20 μM), valinomycin (Val, 25 μM), antimycin (Ant, 25 μM) or azide (250 μM). Values represent average and standard error from 25–35 measurements in each case. Although not shown, the 30 min incubation with each of the inhibitors resulted in 50–55% reduction in cellular ATP levels. (**B**) The state of mitochondrial $\Delta\psi_m$ was tested by staining with cationic fluoresent dye, Mitotracker. (a) control cells; (b) CCCP-treated; (c) valinomycin-treated; (d) antimycin-treated; and (e) azide-treated cells. (**C**–**E**) Western blot analyses of post-nuclear protein fraction (50 μg each) using monospecific antibody to RyR-1, and IP3 channel proteins and plasma membrane Na^+/K^+ ATPase, respectively. The three panels correspond to different regions of a single blot. Details of the Western blot analysis and imaging are described in Materials and methods.

all of the samples (see Figure 6C). The Western blot in Figure 6F shows that the nuclear content of the calcineurin-dependent NFATc is also increased 5- to 6-fold in mtDNA-depleted cells, which returns to near normal levels in reverted cells.

Pro-inflammatory cytokines and UV irradiation activate JNK family protein kinases, which in turn activate ATF2 by Thr phosphorylation (Gupta *et al*., 1995). Western blot in Figure 6G shows the relative levels of the phosphorylated form of ATF2 in the nuclear protein fraction of control and treated cells. Results show that ATF2 is activated in mtDNA-depleted cells by ~7-fold of the control, and the activated ATF2 level returns to near normal in reverted cells. Although results are not presented, JNK1 is also activated in mtDNA-depleted cells. Finally, the relative levels of the ubiquitous transcription factor YY-1 remained nearly the same in all of the cell types. These results collectively demonstrate that mitochondrial stress-mediated retrograde Ca^{2+} signaling affects the activity of some of the key cytosolic regulatory proteins and also the activity of three different inflammatory response transcription factors.

Effects of mitochondrial inhibitors on steady-state $[Ca^{2+}]_i$ and RyR-1 channel protein

We tested a number of mitochondrial inhibitors to ascertain further if disruption of mitochondrial transmembrane potential and inhibition of mitochondrial ATP synthesis affected resting cytoplasmic $[Ca^{2+}]_i$ and Ca^{2+}-dependent gene transcription. Specifically, we chose the mitochondrial-specific ionophore CCCP and a more general ionophore valinomycin, both of which disrupt the mitochondrial membrane potential and inhibit respiration-coupled phosphorylation. We also used antimycin and azide, which block the electron transport chain and coupled proton translocation. In order to be able to see the effects of these agents on transcription upregulation and protein accumulation, we chose a long-term (chronic) treatment of 30 min. Under these conditions, antimycin and azide can also cause mitochondrial membrane depolarization through gradual loss of H^+ gradient because of ongoing mitochondrial transport and normal 'leaks' which can not be corrected.

Results of single cell Ca^{2+} measurements in Figure 7A show that treatment of cells with 20 μM CCCP for 30 min resulted in increased basal $[Ca^{2+}]_i$ to ~165 nM (bar 2) compared with 65 nM in control cells (bar 1). Treatment with 100 μM azide, 25 μM valinomycin and 25 μM antimycin for 30 min also resulted in a 2- to 3-fold elevation of $[Ca^{2+}]_i$ (Figure 7A, bars 3–4). Although not shown, similar to the CCCP-treated control cells in Figure 2A, the ATP levels in these inhibitor-treated cells were reduced to 45–55% of control cells. The state of $\Delta\psi_m$ in these cells was tested by staining with the

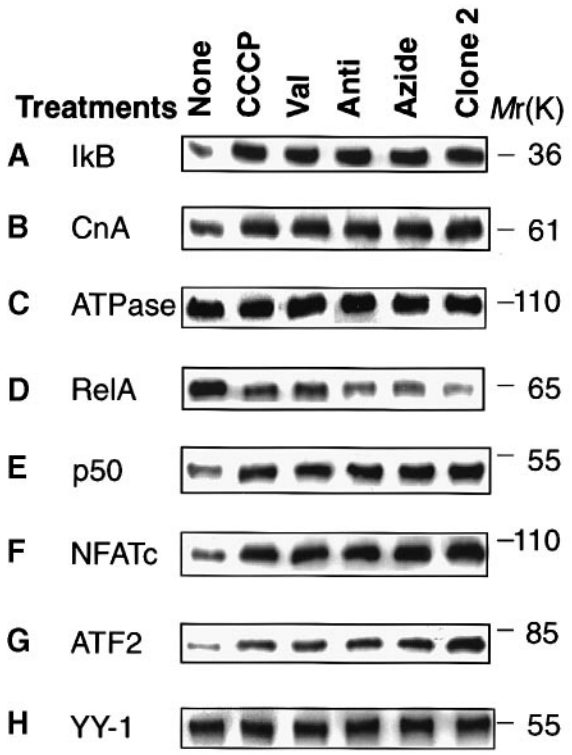

Fig. 8. Effects of mitochondrial metabolic inhibitors on the level of various transcription factors. (**A**–**C**) Western blot analyses of post-mitochondrial protein fractions (50 μg each) from various inhibitor-treated and untreated cells using antibodies to IκB, calcineurin A (CnA) and Na^+/K^+ ATPase (ATPase), respectively. (**D**–**H**) Western blot analyses of nuclear protein fractions (20 μg each) with antibodies to RelA, p50, NFATc, phosphorylated ATF2 and YY-1 as indicated. The concentrations of inhibitors and duration of treatments were similar to those described in Figure 6. Details of the Western blot analysis, imaging and quantitation are described in Materials and methods.

mitochondrial-specific cationic dye, Mitotracker. As shown in Figure 7B, mitochondria-like punctuate structures were able to mobilize the fluorescent dye in normal cells (panel a), while all of the inhibitor-treated cells (panels b–e) show vastly reduced fluorescence, suggesting reduced mitochondrial transmembrane potential. Thus, as observed with mtDNA-depleted cells, loss of transmembrane potential resulting in reduced ATP levels, and associated effects on Ca^{2+} efflux may be reasons for the increased steady-state $[Ca^{2+}]_i$ in these inhibitor-treated cells.

As shown in Figure 7C, the level of RyR-1 antibody-reactive ~500 kDa protein was induced in cells treated with all of the mitochondrial inhibitors which elevated $[Ca^{2+}]_i$. The levels of $InsP_3$ receptor protein (Figure 7D) and Na^+/K^+ ATPase (Figure 7E) remained at control levels. These results are consistent with the possibility that mitochondrial dysfunction results in moderate but sustained elevation of $[Ca^{2+}]_i$, which in turn initiates calcium-dependent changes in nuclear gene expression.

Effects of mitochondrial metabolic stress on Ca^{2+} responsive transcription factors

The similarity between the Ca^{2+} changes in response to mtDNA depletion and mitochondrial metabolic inhibitors, which disrupt $\Delta\psi_m$, was further investigated by assaying the levels of Ca^{2+} responsive transcription factors. Results of the Western blot in Figure 8 show that as seen with the mtDNA-depleted cells, treatment with all four inhibitors resulted in an elevated cytoplasmic IκB and calcineurin A subunit (Figure 8A and B) without any significant change in the Na^+/K^+ ATPase (Figure 8C) used as a loading control. The results also show a reduced nuclear RelA and increased nuclear p50, and NFATc contents and also an increased activated ATF2 protein factors (Figure 8D–G), with no significant change in the level of the ubiquitous nuclear factor YY-1 (Figure 8H). The overall levels of increase or decrease in relation to untreated controls show marginal variations for different inhibitors, although the values are in general agreement with the extent of increase or decrease of the various protein factors seen in similar fractions from mtDNA-depleted clone 2 (Figure 8H, last lanes in A–H).

Discussion

In this study we have used a combination of mtDNA depletion and reversal, as well as mitochondrial metabolic inhibitors, to investigate the nature of the mitochondrial stress signal and how it might be transmitted to the nuclear compartment. Some studies have reported significantly higher steady-state levels of nuclear-encoded mRNAs for some of the mitochondrial proteins in ρ^o cells of human and other metazoan origins (Marusich *et al*., 1997; Wang and Morais, 1997). However, the molecular basis for increased mRNA pools in these studies remain unknown. Irreversibility of the mtDNA content in these ρ^o cells makes it difficult to ascribe a definite mitochondrial lesion as the primary cause of increased mRNA levels. In the case of most ρ^o yeast cells studied, although the bHLH factor involved in the transcriptional upregulation of *CIT 2* gene has been well characterized, the nature of mitochondrial signal which activates the factor remains unknown. We have developed a series of muscle cell lines with partially depleted mtDNA, which can be fully reverted to near normal status. Our results demonstrate that both genetic and metabolic stress in mammalian cells, which disrupt $\Delta\psi_m$ and affect mitochondrial ATP synthesis are transmitted as a retrograde Ca^{2+} signal, which in turn leads to altered nuclear gene expression.

A key observation of this study is that in addition to the nuclear genes involved in mitochondrial biogenesis, the mitochondrial genetic and metabolic stress signal also affects the expression of other cellular genes, such as *RyR-1* Ca^{2+} channel gene. In keeping with this, myocytes subjected to mitochondrial stress released high Ca^{2+} transients in response to caffeine stimulation. Interestingly, transcriptional activation of *RyR-1* gene expression appears to be highly specific, since the expression of *RyR-3* and ubiquitously expressed *IP3R* levels remain unaffected. This makes a biological sense, as an increase in RyR-1 may affect the responsiveness of individual myocytes to external stimuli, including membrane depolarization. It should be noted that the muscle voltage sensor, the dihydropyridine receptor, couples conformationally to the RyR-1 to release Ca^{2+} during muscle contraction. In addition, Ca^{2+} release from the muscle $InsP_3R$ has been shown not to contribute significantly to the contractile response (Walker *et al*., 1987).

We propose that mitochondrial stress may contribute to the elevated $[Ca^{2+}]_i$ indirectly due to reduced Ca^{2+} efflux

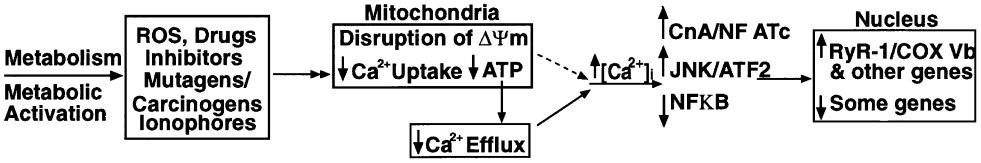

Fig. 9. A proposed model for mitochondrial stress signaling. Mitochondrial metabolism and metabolic activation of O_2, environmental carcinogens and pharmacologically important drugs by various mitochondrial enzymes produce ROS and electrophilic reactive mutagens, which in turn affect mitochondrial gene expression and mitochondrial membrane potential ($\Delta\psi_m$). Long-term exposure to inhibitors of mtDNA replication and gene expression, and inhibitors of electron transport chain complexes also cause a similar end result. An upward arrow in the model indicates a net increase in concentration (such as Ca^{2+} ion), activation of factors, or upregulation of transcription. A downward arrow indicates inactivation of factors, or down regulation of transcription. The model suggests that reduced ATP and reduced Ca^{2+} efflux may be major contributors, while reduced mitochondrial Ca^{2+} uptake may contribute to a lesser extent. CaA, calcineurin; CICR, calcium-induced calcium release.

through the plasma membrane because of reduced ATP levels. The conventional view is that the balance between the Ca^{2+} influx and Ca^{2+} efflux at the plasma membrane is the primary determinant of steady-state $[Ca^{2+}]_i$. However, there is emerging evidence that mitochondria also play a role in sequestering Ca^{2+} from the cytosol, as part of the intracellular Ca^{2+} network. One can not, therefore, ignore the contribution of disrupted $\Delta\psi_m$ to an increase in steady-state $[Ca^{2+}]_i$. It is noteworthy that studies with different cell types (Duchen and Biscoe, 1992; Lou *et al*., 1997) suggest that disruption of $\Delta\psi_m$ by inhibitors cause a marginal to significant increase in $[Ca^{2+}]_i$. A recent study by Babcock *et al*. (1997) showed a rapid Ca^{2+} uptake by mitochondria in response to release from endoplasmic reticular or plasma membrane stores, and a steady release to the cytoplasm through a secondary Na^+/Ca^{2+} active transport system. The buffering effect of mitochondria and its ability to clear Ca^{2+} from the cytoplasm depend on negative $\Delta\psi_m$ and also active Na^+/Ca^{2+} antiport system (Rizzuto *et al*., 1993; Hansford, 1994; Ichas *et al*., 1994, 1997; Hajnoczky *et al*., 1995; Babcock *et al*., 1997).

Ca^{2+}-dependent processes in cells are regulated through the generation of spatially and temporally distinct Ca^{2+} waves including single spikes, repeating oscillations, or sustained low plateaus (Berridge, 1993; Fewtrell, 1993; Clapham *et al*., 1995). Such changes in $[Ca^{2+}]_i$ can affect pro-inflammatory transcription regulatory factors NF-κB, JNK-dependent ATF2, and calcineurin-dependent NFAT are differentially activated (Dolmetsch *et al*., 1997). In further resolution of different modes of Ca^{2+} waves, it has been shown that oscillation amplitude and frequency are the determining factors in the differential activation of transcription factors, and thus regulation of gene expression (Berridge, 1993; Dolmetsch *et al*., 1998; Li *et al*., 1998). We believe that the Ca^{2+} signaling due to mitochondrial stress (depleted $\Delta\psi_m$ and/or reduced ATP levels) is likely to be different from the above described Ca^{2+} signaling modes, since we see a moderate, yet sustained increase in steady-state $[Ca^{2+}]_i$ and a vastly increased RyR-1-mediated Ca^{2+} release in stressed C2C12 myocytes. Our results also show that under the mitochondrial stress conditions, transcription factors belonging to two distinct pathways, namely, calcineurin dependent-NFATc and JNK-dependent ATF2 are activated, while NF-κB (Rel A) is inactivated.

As shown in the working model in Figure 9, we postulate that chemical, oxidative and other metabolic stresses that inflict changes in $\Delta\psi_m$ and thus the cellular ATP level results in a moderate, but sustained elevation of $[Ca^{2+}]_i$. The latter in turn leads to activation of calcineurin and JNK pathways and inactivation of NF-κB. We believe that altered $\Delta\psi_m$ and its associated decrease in ATP is the primary signal for the cascade. The observed upregulation of the *RyR-1* gene and mitochondrial-destined *COX Vb* gene expression may be immediate consequences of these altered transcription factors. Preliminary results (data not shown) show that the mouse *COX Vb* promoter (Lenka *et al*., 1998), is transcriptionally activated by NFATc/AP1 factors and human *RYR-1* proximal promoter (Phillips *et al*., 1996) is activated by a combinatorial effect of NF-κB family and ATF2 transcription factors. Results of the differential display of mRNA (data not shown) from mtDNA-depleted C2C12 cells also suggest that the retrograde Ca^{2+} signaling may affect the expression of $<$15 nuclear genes which encode proteins with various cellular function, including mitochondrial biogenesis.

Mitochondrial membrane biogenesis involves a co-ordinated regulation of mitochondrial gene expression and the expression of well over 100 nuclear genes encoding various mitochondrial proteins (Attardi and Schatz, 1988; Poyton and McEwen, 1996). Currently, a number of different hypotheses exist on the intergenic regulation of mitochondrial biogenesis. Studies in different cell types have indirectly suggested different mechanisms of intergenic crosstalk, including O_2 tension, reactive O_2 species (ROS) (Poyton and McEwen, 1996) and use of common transcription factors which might coordinate the nuclear and mitochondrial transcription rates (Nagley, 1991; Virbasius and Scarpulla, 1994; Larsson *et al*., 1996; Lenka *et al*., 1998). However, despite intensive efforts, the precise means of intergenic crosstalk remain unclear. Our results show that at least one such long sought-after means of inter-organelle communication involves the intracellular Ca^{2+} network (see Figure 9). Furthermore, a modest reduction (20% reduction) in mtDNA content resulting in ~20–25% lower ATP levels, is sufficient to activate the stress signal suggesting its physiological significance in various myopathies and mitochondrial dysfunctional diseases. Currently, there is compelling evidence that the mitochondrial system is highly sensitive to both oxidative and chemical stress; mitochondria produce ROS under certain physiological conditions, but also metabolically activate xenobiotic chemicals to reactive electrophilic compounds (Niranjan *et al*., 1982; Wallace, 1992; Larsson and Clayton, 1995; Addya *et al*., 1997; Pinz and Bogenhagen, 1998). Of particular significance from these findings is that the retrograde Ca^{2+} signaling affects not only genes involved in mitochondrial biogenesis, but also those with functions in other cellular processes, including Ca^{2+} homeostasis.

Our results also have important implications in understanding the molecular mechanisms of various mitochondrial diseases. It is generally believed that lowered electron transport rate and low mitochondrial energy coupling may be key factors in the manifestation of various mitochondrial dysfunctional diseases. Our results imply that altered Ca^{2+} homeostasis and altered nuclear gene expression patterns may also be important factors in the clinical onset of the disease. This interpretation is consistent with observations that cardiac muscle myopathies and age-related neural degeneration are associated with cellular Ca^{2+} loading (Peterson and Goldman, 1986; Di Lisa *et al*., 1993; McCoy *et al*., 1993; Hansford, 1994) and suspected changes in intracellular Ca^{2+} pools.

Materials and methods

Cell system and isolation of clones

C2C12 mouse skeletal muscle cells were grown in high glucose, Dulbecco's modified Eagle's medium (DMEM) supplemented with 10% heat inactivated fetal bovine serum (FBS) and 0.1% gentamycin. Cells were grown in the presence of 100 ng/ml of EtBr for 70 passages, and trypsinized cells were serially diluted and plated at a density of ~100 cells/plate. After 10–15 days of growth, individual colonies were selected with the help of glass-cloning cylinders and screened for mtDNA content by Southern hybridization described below. Cells from 30 individual clones were grown in the FBS-supplemented DMEM with added 1 mM pyruvate and 50 μg/ml uridine in the presence of EtBr, and frozen as aliquots in liquid nitrogen. In all the experiments described in this paper, 1×10^6 cells from this initial frozen stock were grown to ~80% confluency in the pyruvate/uridine-supplemented medium in the presence of added EtBr (100 ng/ml). The frozen stocks required a maximum of 4 days of growth to reach confluency. In addition, the mtDNA contents of the clones used in this study were tested periodically by Southern hybridization, and the mtDNA contents were within the 96–102% range of the respective parent clones. In some experiments, 80% confluent cells were grown for an additional 48 h in the absence of FBS but in the presence of EtBr to induce myogenesis.

Determination of mtDNA contents

Cells (20×10^6/ml in 10 mM Tris–HCl pH 8.0, 100 mM NaCl, 25 mM EDTA) were lysed with 0.5% SDS and digested with 0.1 mg/ml of pronase for 18 h. Following digestion with DNase-free RNase, total DNA was isolated either by phenol/chloroform extraction or CsCl banding. Total cell DNA (0.5 μg) was digested with *Bgl*II to linearize the 15.28 kb mouse mtDNA. The resultant DNA was analyzed by Southern blot hybridization with 5′ end labeled synthetic DNA sequence (5′-AATGTGTGATATGGTGGAGGGCATCC-3′) from the mouse *COX I* gene. The blots were also hybridized with an 18S rRNA-specific DNA probe. The blots were quantitated in a Bio-Rad GS-525 imager and the values were normalized to the 18S DNA contents of the respective samples.

Immunocytochemistry and fluorescence microscopy

Cells were grown on coverslips, and processed for antibody staining essentially as described (Addya *et al*., 1997). Cells were fixed with 2% paraformaldehyde permeabilized with 0.1% Triton X-100 and blocked with 5% goat serum for 1 h at 25°C. Cells were immunostained with 1:100 dilution of primary antibody. Cells were washed four times with phosphate-buffered saline (PBS) to remove unbound antibody and incubated with 1:100 dilutions of fluorescein isothiocyanate-conjugated anti-rabbit or anti-mouse antibodies (Jackson Immuno Research laboratories, Inc., West Grove, PA), for 1 h at 37°C. Unbound secondary antibodies were removed by repeated washing with PBS. Fluorescence microscopy was carried out under a TCS laser scanning microscope (Leica Inc., Deerfield, IL). Optical sections of 0.5 μm were scanned at the *z*-axis. Affinity-purified rabbit polyclonal antibodies against purified RyR-1 or IP3 proteins (Zaidi *et al*., 1995), or monoclonal antibody against human COX I protein (Molecular Probes, Inc.) were used.

Staining with the cationic fluorescent dye, Mitotracker, was carried out by the same procedure, except that unfixed live cells were loaded with 400 nM Mitotracker (Molecular Probes, Inc.) for 45 min at 37°C. The cells were briefly rinsed with PBS and fixed with 2% paraformaldehyde for 20 min. The excess dye was removed by washing with PBS and cells were viewed through a Leica confocal microscope described above.

Single cell $[Ca^{2+}]_i$ measurements

Glass coverslips containing C1C2 cells were incubated in serum-free physiological medium (30 min, 37°C) with 10 μM fura-2/AM (Molecular Probes, San Diego, CA), then washed in M199-H and transferred to a Perspex bath positioned on the microspectrofluorimeter stage. The latter was previously constructed from an inverted microscope (Diaphot, Nikon, Telford, UK) (Shankar *et al*., 1993). The cells were exposed alternately to excitation wavelengths of 340 or 380 nm. The emitted fluorescence was deflected through a 400 nm dichroic mirror and subsequently filtered at 510 nm. An intensified CCD camera was used for imaging (Ion Optix, Worster, MA). Image intensities were recorded every second to give a ratio of emitted intensities at excitation wavelengths of 340 and 380 nm, F_{340}/F_{380}. The cytosolic Ca^{2+} measuring system was calibrated using an established protocol for intracellular calibration (Shankar *et al*., 1993). Briefly, fura-2-loaded myocytes were bathed in Ca^{2+}-free, EGTA-containing solution containing 130 mM NaCl, 5 mM KCl, 5 mM glucose, 1 mM pyruvate, 50 μg/ml uridine, 0.8 mM $MgCl_2$, 10 mM HEPES and 0.1 mM EGTA. Ionomycin (5 μM) was first applied to obtain the minimum ratio due to lowest cytosolic Ca^{2+} (R_{min}) and the maximum fluorescence intensity at 380 nm (Sf2). $CaCl_2$ (1 mM) was then applied with 5 μM ionomycin to obtain values of the maximum ratio due to an elevated cytosolic Ca^{2+} (R_{max}) and the minimum fluorescence intensity at 380 nm (Sb2). The dissociation constant K_d for Ca^{2+} and fura-2 is 224 nM (20°C, 0.1 M, pH = 6.85). The values were substituted into the equation: $[Ca^{2+}] = K_d\times[(R - R_{min})/(R_{max} - R)]\times[(Sf2/Sb2)]$. Mean changes (Δ) in the cytosolic Ca^{2+} concentration ($[Ca^{2+}]$) were then calculated by subtracting peak from basal cytosolic $[Ca^{2+}]$. Statistical comparisons of cytosolic Δ $[Ca^{2+}]$ were made by ANOVA with Bonferroni's Correction for Inequality.

Western blot analysis

Cells were homogenized in 0.3 M sucrose, 10 mM Tris–HCl pH 8.0, 10 mM NaCl, 3 mM $MgCl_2$, 1 mM $NaVO_4$, 100 μM molybdic acid, 10 mM NaF, 0.2 mM EDTA, 1 mM phenylmethylsulfonyl fluoride, 50 μg/ml each leupeptin, pepstatin, aprotinin, chymostatin and antipain in a Dounce homogenizer (A type pestle), and centrifuged at 1500 *g* for 5 min at 4°C. The nuclear pellet was washed with the same buffer containing 0.5% Nonidet P40, lysed in a hypotonic buffer and centrifuged at 25 000 *g* for 10 min to remove the chromatin fraction. The resulting supernatant was used as the nuclear protein fraction. The 1500 *g* supernatant from the initial spin was further centrifuged at 10 000 *g* for 10 min at 4°C to remove heavy mitochondrial membrane. Supernatant from this spin, used as the total cytoplasmic fraction, also contained endoplasmic reticulum and plasma membrane fractions. Proteins resolved on polyacrylamide gels were subjected to Western blot analysis using affinity-purified antibodies for RyR-1 and IP3 receptor proteins (Zaidi *et al*., 1995). Antibodies for IκB, Rel A and Na^+/K^+ ATPase were purchased from Santa Cruz Biotechnology Inc. Antibodies to murine calcineurin A and B subunits were purchased from Sigma chemical Co. and Affinity BioReagents Inc., respectively. Antibodies highly specific for the phosphorylated ATF2 protein was purchased from New England Biolabs Inc. Polyclonal antibody to human YY-1 was a generous gift from Dr Michael Atchison. The immunoblots were developed using the Pierce Super Signal ULTRA chemiluminescent substrate kit, imaged and quantitated in a Bio-Rad Fluor-S imaging system.

Measurement of cellular ATP levels

ATP levels were measured using a somatic cell ATP assay kit (Sigma Chemical Co., St Louis, MO), which is based on the assay of ATP-driven luciferin luciferase activity (Strehler, 1968). Cells harvested at 4–6°C were lysed with the 'ATP releasing reagent' and the lysates were assayed for luciferase activity as per the manufacturer's procedure in a TD-20/20 Luminometer (Turner Designs, Sunnyvale, CA), using appropriate controls and blanks. Respiration-coupled ATP was measured indirectly as CCCP or oligomycin-sensitive components. In these experiments cells were pretreated with 20 μM CCCP or 25 μM oligomycin for 30 min before the assay.

Reverse transcription-based PCR

Total cell RNA (2.5 μg) was reverse transcribed using appropriate reverse primers, and subsequently amplified by PCR using an RT–PCR kit from Perkin Elmer/ABI. RyR-1 specific reverse primer (5′-CACCTGCTGGACATCGCCATGGG-3′, sequence 14434–14457), and

forward primer (5′-ATGTAATTGGCCAGATTGTGCTC-3′, sequence 14994–14967) which is conserved among human, rabbit and pig; or a set of degenerate primers that amplify RyR-1, RyR2, as well as RyR3 mRNAs (Bennett *et al*., 1996) were used. The mouse mtTFA mRNA was amplified using a sense primer (5′-TACCCAAAGAAACCTATGAGT-3′) and an anti-sense primer (5′-CATTTGTTCTTCCCAAGACTTC-3′) which yield a 500 bp DNA product (Larsson *et al*., 1996).

Acknowledgements

We thank Drs Michael Atchison, David F.Wilson, Lee Sweeney, June Aprille, Jorge Caamano and F.Anthony Lai for critical comments on the manuscript and for generously providing some of the antibodies used in this study. We also thank members of the Avadhani laboratory for help and suggestions, and Dr Lee Peechy and Ms Gladys Gray-Board for the use of the confocal microscopy facility. This work was supported in part by NIH grant CA-22762-21 to N.G.A. and AG14917-02 to M.Z.

References

Addya,S., Anandatheerthavarada,H.K., Biswas,G., Bhagwat,S.V., Mullick,J. and Avadhani,N.G. (1997) Targeting of NH_2-terminal-processed microsomal protein to mitochondria: a novel pathway for the biogenesis of hepatic mitochondrial P450MT2. *J. Cell Biol*., **139**, 589–599.

Altschuld,R.A., Hohl,C.M., Castillo,L.C., Garleb,A.A., Starling,R.C. and Brierley,G.P. (1992) Cyclosporin inhibits mitochondrial calcium efflux in isolated adult rat ventricular cardiomyocytes. *Am. J. Physiol*., **262**, H1699–H1704.

Arnheim,N. and Cortopassi,G. (1992) Deleterious mitochondrial DNA mutations accumulate in aging human tissues. *Mutat. Res.*, **275**, 157–167.

Attardi,G. and Schatz,G. (1988) Biogenesis of mitochondria. *Annu. Rev. Cell Biol*., **4**, 289–333.

Babcock,D.F., Herrington,J., Goodwin,P.C., Park,Y.B. and Hille,B. (1997) Mitochondrial participation in the intracellular Ca^{2+} network. *J. Cell Biol*., **136**, 833–844.

Barath,Z. and Kuntzel,H. (1972) Induction of mitochondrial RNA polymerase in *Neurospora crassa*. *Nature New Biol*., **240**, 195–197.

Bennett,D.L., Cheek,T.R., Berridge,M.J., De Smedt,H., Parys,J.B., Missiaen,L. and Bootman,M.D. (1996) Expression and function of ryanodine receptors in nonexcitable cells. *J. Biol. Chem*., **271**, 6356–6362.

Berridge,M.J. (1993) Inositol triphosphate and calcium signaling. *Nature*, **361**, 315–325.

Capaldi,R.A. (1990) Structure and function of cytochrome c oxidase. *Annu. Rev. Biochem*., **59**, 569–596.

Carafoli,E. (1979) The calcium cycle of mitochondria. *FEBS Lett*., **104**, 1–5.

Chen,L.B. (1989) Fluorescent labeling of mitochondria. *Methods Cell Biol*., **29**, 103–123.

Clapham,D.E. (1995) Calcium signaling. *Cell*, **80**, 259–268.

Corral-Debrinski,M., Horton,T., Lott,M.T., Shoffner,J.M., Beal,M.F. and Wallace,D.C. (1992) Mitochondrial DNA deletions in human brain: regional variability and increase with advanced age. *Nature Genet*., **2**, 324–329.

Davis,R.E. *et al*. (1997) Mutations in mitochondrial cytochrome c oxidase genes segregate with late-onset Alzheimer's disease. *Proc. Natl Acad. Sci. USA*, **94**, 4526–4531.

Desjardins,P., de Muys,J.M. and Morais,R. (1986) An established avian fibroblast cell line without mitochondrial DNA. *Somatic. Cell Mol. Genet*., **12**, 133–139.

Di Lisa,F., Fan,C.-Z., Gambassi,G., Hogue,B., Kudryashova,I. and Hansford,R. (1993) Altered pyruvate dehydrogenase control and mitochondrial free Ca^{2+} in hearts of cardiomyopathic hamsters. *Am. J. Physiol*., **264**, H2188–H2197.

DiMauro,S. (1993) Mitochondrial encephalopathies. *Arch. Neurol*., **50**, 1197–1208.

DiMauro,S. (1996) Mitochondrial encephalomyopathies: what next? *J. Inher. Met. Dis.*, **19**, 489–503.

Dolmetsch,R.E., Lewis,R.S., Goodnow,C.C. and Healy,J.I. (1997) Differential activation of transcription factors induced by Ca^{2+} response amplitude and duration. *Nature*, **386**, 855–858.

Dolmetsch,R., Xu,K. and Lewis,R. (1998) Calcium oscillations increase the efficiency and specificity of gene expression. *Nature*, **392**, 933–936.

Duchen,M. and Biscoe,T. (1992) Relative mitochondrial membrane potential and $[Ca^{2+}]_i$ in type I cells isolated from the rabbit carotid body. *J. Physiol*., **450**, 33–61.

Fan,C. and Maniatis,T. (1991) Generation of p50 subunit of NFκB by processing of p105 through an ATP dependent pathway. *Nature*, **354**, 395–398.

Fewtrell,C. (1993) Ca^{2+} oscillations in non-excitable cells. *Annu. Rev. Physiol*., **55**, 427–454.

Friel,D.D. and Tsien,R.W. (1994) An FCCP-sensitive Ca^{2+} store in bullfrog sympathetic neurons and its participation in stimulus-evoked changes in $[Ca^{2+}]_i$. *J. Neurosci*., **14**, 4007–4024.

Grassi,F., Giovannelli,A., Fucile,S. and Eusebi,F. (1993) Activation of the nicotinic acetylcholine receptor mobilizes calcium from caffeine-insensitive stores in C2C12 mouse myotubes. *Pflugers Arch*., **422**, 591–598.

Grilli,M., Chiu,J.J. and Lenardo,M.J. (1993) NFκB and Rel: participants in a multiform transcriptional regulation system. *Int. Rev. Cytol*., **143**, 1–62.

Gupta,S., Campbell,D., Derijard,B. and Davis,R.J. (1995) Transcription factor ATF2 regulation by the JNK signal transduction pathway. *Science*, **267**, 389–393.

Hajnoczky,G., Robb-Gaspers,L.D., Seitz,M.B. and Thomas,A.P. (1995) Decoding of cytosolic calcium oscillations in the mitochondria. *Cell*, **82**, 415–424.

Hansford,R. (1994) Physiological role of mitochondrial Ca^{2+} transport. *J. Bioenerg. Biomembr*., **26**, 495–508.

Hayakawa,M., Hattori,K., Sugiyama,S. and Ozawa,T. (1992) Age-associated oxygen damage and mutations in mitochondrial DNA in human hearts. *Biochem. Biophys. Res. Commun*., **189**, 979–985.

Holt,I.J., Harding,A.E. and Morgan-Hughes,J.A. (1988) Deletions of muscle mitochondrial DNA in patients with mitochondrial myopathies. *Nature*, **331**, 717–719.

Ichas,F., Jouaville,L.S., Sidash,S.S. Mazat,J.-P. and Holmuhamedov,E.L. (1994) Mitochondrial calcium spiking: a transduction mechanism based on calcium-induced permeability transition involved in cell calcium signaling. *FEBS Lett*., **348**, 211–215.

Ichas,F., Jouaville,L.S. and Mazat,J.P. (1997) Mitochondria are excitable organelles capable of generating and conveying electrical and calcium signals. *Cell*, **89**, 1145–1153.

Jia,Y., Rothermel,B., Thornton,J. and Butow,R.A. (1997) A basic helix–loop–helix leucine zipper heterodimer in yeast functions in a signaling pathway from mitochondria to the nucleus. *Mol. Cell. Biol*., **17**, 1110–1117.

King,M. and Attardi,G. (1989) Human cells lacking mtDNA: repopulation with exogenous mitochondria by complementation. *Science*, **246**, 500–503.

Kuiper,M.T., Akins,R.A., Holtrop,M., de Vries,H. and Lambowitz,A.M. (1988) Isolation and analysis of the *Neurospora crassa* Cyt-21 gene. A nuclear gene encoding a mitochondrial ribosomal protein. *J. Biol. Chem*., **263**, 2840–2847.

Larsson,N.-G. and Clayton,D.A. (1995) Molecular genetic aspects of human mitochondrial disorders. *Annu. Rev. Genet*., **29**, 151–178.

Larsson,N.G., Garman,J.D., Oldfors,A., Barsh,G.S. and Clayton,D.A. (1996) A single mouse gene encodes the mitochondrial transcription factor A and a testis-specific nuclear HMG-box protein. *Nature Genet*., **13**, 296–302.

Lenka,N., Vijayasarathy,C., Mullick,J. and Avadhani,N.G. (1998) Structural organization and transcription regulation of nuclear gene encoding the mammalian cytochrome *c* oxidase complex. *Progr. Nucleic Acid Res. Mol. Biol*., **61**, 309–344.

Li,W.-h., Liopis,J., Whitney,M., Zlokarnik,G. and Tsien,R. (1998) Cell-permeant caged InsP3 ester shows that Ca^{2+} spike frequency can optimize gene expression. *Nature*, **392**, 936–941.

Liao,X. and Butow,R.A. (1993) RTG1 and RTG2: two yeast genes required for a novel path of communication from mitochondria to the nucleus. *Cell*, **72**, 61–71.

Liu,J., Farmer,J.D.,Jr, Lane,W.S., Friedman,J., Weissman,I. and Schreiber,S.L. (1991) Calcineurin is a common target of cyclophilin–cyclosporin A and FKBP–FK506 complexes. *Cell*, **66**, 807–815.

Loew,L.M., Carrington,W., Tuft,R.A. and Fay,F.S. (1994) Physiological cytosolic Ca^{2+} transients evoke concurrent mitochondrial depolarizations. *Proc. Natl Acad. Sci. USA*, **91**, 12579–12583.

Lou,Y., Bond,J. and Ingram,V.M. (1997) Compromised mitochondrial functions leads to increased cytosolic calcium and activation of MAP kinases. *Proc. Natl Acad. Sci. USA*, **94**, 9705–9710.

Marusich,M.F., Robinson,B.H., Taanman,J.W., Kim,S.J., Schillace,R., Smith,J.L. and Capaldi,R.A. (1997) Expression of mtDNA and nDNA encoded respiratory chain proteins in chemically and genetically-

derived Rho0 human fibroblasts: a comparison of subunit proteins in normal fibroblasts treated with ethidium bromide and fibroblasts from a patient with mtDNA depletion syndrome. *Biochim. Biophys. Acta*, **1362**, 145–159.

McCoy,K.R., Mullins,R.D., Newcomb,T.G., Ng,G.M., Pavlinkova,G., Polinsky,R.J., Nee,L.E. and Sisken,J.E. (1993) Serum- and bradykinin-induced calcium transients in familial Alzheimer's fibroblasts. *Neurobiol. Ageing*, **14**, 447–455.

Milan,D., Griffith,J., Su,M., Price,E.R. and McKeon,F. (1994) The latch region of calcineurin B is involved in both immunosuppressant–immunophilin complex docking and phosphatase activation. *Cell*, **79**, 437–447.

Molkentin,J.D., Lu,J.R., Antos,C.L., Markham,B., Richardson,J., Robbins,J., Grant,S.R. and Olsen,E.N. (1998) A calcineurin-dependent transcriptional pathway for cardiac hypertrophy. *Cell*, **93**, 215–228.

Moraes,C.T. *et al*. (1989) Mitochondrial DNA deletions in progressive external ophthalmoplegia and Kearns–Sayre syndrome. *New Eng. J. Med.*, **320**, 1293–1299.

Nagley,P. (1991) Coordination of gene expression in the formation of mammalian mitochondria. *Trends Genet.*, **7**, 1–4.

Nass,M.M. (1972) Differential effects of ethidium bromide on mitochondrial and nuclear DNA synthesis *in vivo* in cultured mammalian cells. *Exp. Cell Res.*, **72**, 211–222.

Niranjan,B.G., Bhat,N.K. and Avadhani,N.G. (1982) Preferential attack of mitochondrial DNA by aflatoxin B1 during hepatocarcinogenesis. *Science*, **215**, 73–75.

O'Keefe,S.J., Tamura,J., Kincaid,R.L., Tocci,M.J. and O'Neill,E.A. (1992) FK-506- and CsA-sensitive activation of the interleukin-2 promoter by calcineurin. *Nature*, **357**, 692–694.

Parikh,V.S., Morgan,M.M., Scott,R., Clements,L.S. and Butow,R.A. (1987) The mitochondrial genotype can influence nuclear gene expression in yeast. *Science*, **235**, 576–580.

Peterson,C. and Goldman,J.E. (1986) Alterations in calcium content and biochemical processes in cultured skin fibroblasts from aged and Alzheimer donors. *Proc. Natl Acad. Sci. USA*, **83**, 2758–2762.

Phillips,M.S., Fujii,J., Khanna,V.K., DeLeon,S., Yokobata,K., de Jong,P.J. and MacLennan,D.H. (1996) The structural organization of the human skeletal muscle ryanodine receptor (RYR-1) gene. *Genomics*, **34**, 24–41.

Pinz,K.G. and Bogenhagen,D. (1998) Efficient repair of abasic sites in DNA by mitochondrial enzymes. *Mol. Cell. Biol.*, **18**, 1257–1265.

Poyton,R.O. and McEwen,J.E. (1996) Crosstalk between nuclear and mitochondrial genomes. *Annu. Rev. Biochem.*, **65**, 563–607.

Rizzuto,R., Brini,M., Murgia,M. and Pozzan,T. (1993) Microdomains with high Ca^{2+} close to IP3-sensitive channels that are sensed by neighboring mitochondria. *Science*, **262**, 744–747.

Rothermel,B.A., Shyjan,A.W., Etheredge,J.L. and Butow,R.A. (1995) Transactivation by Rtg1p, a basic helix–loop–helix protein that functions in communication between mitochondria and the nucleus in yeast. *J. Biol. Chem.*, **270**, 29476–29482.

Sen,R. and Baltimore,D. (1986) Inducibility of kappa immunoglobulin enhancer-binding protein NFκB by a posttranslational mechanism. *Cell*, **47**, 921–928.

Shankar,G., Davison,I., Helfrich,M.H., Mason,W.T. and Horton,M.A. (1993) Integrin receptor-mediated metabolism of intracellular calcium in rat osteoclasts. *J. Cell Sci.*, **105**, 61–68.

Shibasaki,F. and McKeon,F. (1995) Calcineurin functions in Ca^{2+}-activated cell death in mammalian cells. *J. Cell Biol.*, **131**, 735–743.

Shibasaki,F., Price,E., Milan,D. and McKeon,F. (1996) Role of kinases and the phospahatase calcineurin in the nuclear shuttling of transcription factor NF-AT4. *Nature*, **382**, 370–373.

Strehler,B.L. (1968) Bioluminescence assay: principles and practice. *Methods Biochem. Anal.*, **16**, 99–181.

Takeshima,H. *et al*. (1989) Primary structure and expression from complementary DNA of skeletal muscle ryanodine receptor. *Nature*, **339**, 435–445.

Virbasius,J.V. and Scarpulla,R.C. (1994) Activation of the human mitochondrial transcription factor A gene by nuclear respiratory factors: a potential regulatory link between nuclear and mitochondrial gene expression in organelle biogenesis. *Proc. Natl Acad. Sci. USA*, **91**, 1309–1313.

Walker,J.W., Somlyo,A.V., Goldman,Y.E., Somlyo,A.P. and Trentham,D.R. (1987) Kinetics of smooth and skeletal muscle activation by laser pulse photolysis of caged inositol, 1,4,5-trisphosphate. *Nature*, **327**, 249–252.

Wallace,D. (1992) Diseases of the mitochondrial DNA. *Annu. Rev. Biochem.*, **61**, 1175–1212.

Wallace,D.C., Singh,G., Lott,M.T., Hodge,J.A., Schurr,T.G., Lezza,A.M., Elsas,L.J. and Nikoskelainen,E.K. (1988) Mitochondrial DNA mutation associated with Leber's hereditary optic neuropath. *Science*, **242**, 1427–1430.

Wang,H. and Morais,R. (1997) Up-regulation of nuclear genes in response to inhibition of mitochondrial DNA expression in chicken cells. *Biochim. Biophys. Acta*, **1352**, 325–334.

Zaidi,M. *et al*. (1995) A ryanodine receptor-like molecule expressed in the osteoclast plasma membrane functions in extracellular Ca^{2+} sensing. *J. Clin. Invest.*, **96**, 1582–1590.

Received August 26, 1998; revised November 4, 1998; accepted November 27, 1998